Journal of the mechanical behavior of biomedical materials 69 (2017) 267–274

Contents lists available at ScienceDirect

Journal of the Mechanical Behavior of Biomedical Materials

journal homepage: www.elsevier.com/locate/jmbbm

Research Paper

Effect of root morphology on the susceptibility of endodontically treated teeth to vertical root fracture: An *ex-vivo* model

Raphael Pilo[a,*], Zvi Metzger[b,c], Tamar Brosh[c]

[a] Department of Oral Rehabilitation, The Maurice and Gabriela Goldschleger School of Dental Medicine, Tel Aviv University, Tel Aviv 6997801, Israel
[b] Department of Endodontology, The Maurice and Gabriela Goldschleger School of Dental Medicine, Tel Aviv University, Tel Aviv 6997801, Israel
[c] Department of Oral Biology, The Maurice and Gabriela Goldschleger School of Dental Medicine, Tel Aviv University, Tel Aviv 6997801, Israel

ARTICLE INFO

Keywords:
Vertical root fracture
Strength
Bursting pressure
Morphometric parameters
Cracks

ABSTRACT

Vertical root fracture (VRF) of endodontically treated teeth is relatively common, and the involved teeth have a poor prognosis. Previous destructive methodologies applied force to the root in an uneven manner; thus, the associated experiments could not truly assess the mechanical behavior of VRF. This problem was resolved in the current study via the novel application of a bursting pressure methodology to endodontically treated maxillary central incisors and premolars. Hydrostatic pressure was applied inside the root canal through a cannula bonded to the coronal access cavity, and the apical foramen was sealed. VRFs were observed as water burst from the fractured root surface. Morphometric parameters were measured by staining and serially sectioning the roots. The bursting pressure was significantly lower in the premolars compared with that in the incisors (19.1 ± 3.3 MPa and 25.5. ± 4.5 MPa, respectively, p=0.001). Cracks in the roots appeared from the apex to the cement enamel junction (CEJ) (61%), apex to mid-root (26%) and mid-root to CEJ (13%), and they involved either two root surfaces (52%) or one root surface (48%) and closely resembled clinical VRF cases. Positive correlations were found between the bursting pressure and the proximal root wall thickness, whereas correlations were not observed between the bursting pressure and the buccal or lingual wall thicknesses. Statistical Analyses of Covariance (ANCOVA) models showed that the proximal wall thickness and an elliptically shaped root cross section were the variables that indicated the differences in strength between premolars, which are more prone to VRF, and maxillary central incisors, which are less prone to VRF.

1. Introduction

Roots of endodontically treated teeth are prone to cracks or fractures, and vertical root fracture (VRF) is the most common (Seo et al., 2012). VRF is defined as a longitudinal fracture that is confined to the root and involves one or two aspects. The fracture is usually initiated from the internal canal wall at any level and extends outward to the root surface (Haueisen et al., 2013). The mechanical properties of the root dentine as well as the root morphology are considered the key factors that influence the occurrence of VRF (Kinney et al., 2003; Lertchirakarn et al., 2003a, 2003b).

Universal mechanical testing of dentin, such as 3-point bending, has been conducted on specimens with standard geometries. This approach is unlikely to assess the mechanical behavior of the entire root due to the inhomogeneity and anisotropy as well as the complex spatial and anatomical variations (Tamse et al., 2000; Xu et al., 2014). Moreover, even when a fracture mechanics approach replaces strength as an engineering quantity, beam shaped specimens will still be required and will possess the same limitations (Kinney et al., 2003). Thus, attempts to assess the strength properties of the entire root from data that have been generated from isolated small dentine specimens is an approach that presents major interpretative limitations because of chemical (Rivera and Yamauchi, 1993), ultrastructural (Brauer et al., 2010) and anatomical (Bellucci and Perrini, 2002; Pilo et al., 1987) variations.

Attempts to test the strength of the roots as an entire anatomic structure or compare the strength of different tooth types were previously performed by destructive methodologies that included increased load to failure experiments. The loads were applied either externally on the canal orifice (Capar et al., 2014; El Nasr and El Kader, 2014; Nur et al., 2015; Uzun et al., 2015) or internally within the canal space using hand spreaders (Lertchirakarn et al., 1999, 2003a; Lindauer et al., 1989; Sathorn et al., 2005a). The root strength measured by this latter methodology yielded load values at fracture in various groups of teeth and produced a ratio of 3–9 between the highest and lowest reported values (Holcomb et al., 1987;

* Corresponding author.
E-mail addresses: rafipilo@post.tau.ac.il (R. Pilo), metzger.zvi@gmail.com (Z. Metzger), tbrosh@post.tau.ac.il (T. Brosh).

http://dx.doi.org/10.1016/j.jmbbm.2017.01.017
Received 9 November 2016; Received in revised form 25 December 2016; Accepted 11 January 2017
Available online 12 January 2017
1751-6161/

Lertchirakarn et al., 1999; Pitts et al., 1983). This large range reflects the variability as well as issues with the experimental methodology, which uses spreaders applied at different locations within the root canal to create wedging stresses (Lindauer et al., 1989), thereby transferring the force unevenly to the root walls. Consequently, an evaluation of the mean load at the fracture of different root types (*i.e.,* maxillary incisor *vs*. premolar) indicated that the smallest mesial-distal diameter of the canal was (premolars) more sensitive to wedging stresses and resulted in the lowest load to failure. Indeed, the mean load at fracture was reported to be twofold higher for the central incisors compared with that for the premolars (Lertchirakarn et al., 1999).

Clinical observations have shown that most teeth extracted because of VRF were endodontically treated and more prevalent in elderly people than in young people (Mireku et al., 2010; Yoshino et al., 2014). VRF occurred more often in oval-shaped roots, such as in premolars and the mesial roots of molars (Seo et al., 2012; Tamse et al., 1999; Yoshino et al., 2014). The main direction of crack propagation and fracture was in the buccal-lingual plane (Haueisen et al., 2013; Lertchirakarn et al., 1999; Meister et al., 1980; Sugaya et al., 2015; Tamse et al., 1999).

Attempts to correlate the morphometric parameters of simulated root sections and susceptibility to VRF have only been performed using finite element modeling/finite element analysis (FEM/FEA) (Lertchirakarn et al., 2003a, 2003b; Sathorn et al., 2005b). Such models indicated that the factors that potentially influenced the susceptibility of the roots to VRF included the root canal shape, external root morphology and dentin thickness. These studies demonstrated that when the root canal shape or the external root morphology was oval instead of circular, the intra-canal stress distribution became asymmetrical and presented a tendency for the highest stresses to occur in the buccal-lingual direction on the inner-canal wall. Thus, fracture may be initiated from the site of the greatest curvature of the root canal wall and propagate to the outer root surface. These models indicated that a reduced proximal dentin thickness increased the magnitude but did not affect the direction of the maximal intra-canal tensile stress (Lertchirakarn et al., 2003a, 2003b). Using a 2-dimensional fracture mechanics analysis model, Chai and Tamse (2015) recently supported this finding and extended that explanation to roots with 2 canals that were connected by an isthmus. Hence, these models indicate that VRF occurs when failure conditions are met, mainly as a result of asymmetrical stress concentrations.

Nevertheless, FEA models have their own limitations, such as a dependence on model type, including 2-D, axial symmetric or 3-D models (Meira et al., 2008), inaccurate definitions of the mechanical properties of the tissues, which are usually defined as homogenous and isotropic (Sathorn et al., 2005b), and the difficulty to express the complex spatial and anatomic variations of the roots. Unfortunately, as there is no systematic approach to model VRF, validating the results of such finite element models by direct experimental methodologies that are related to the morphometric parameters of the root canal and the predisposition to VRF is needed and have not been previously reported.

In the present study, a bursting pressure methodology was applied to validate the results of the abovementioned FEA and mathematical models. The bursting pressure method was previously used to test the strength of bovine caudal discs (Schechtman et al., 2006), the anastomotic strength of the colon (Eker et al., 2015; Fallon et al., 2014; Ikeuchi et al., 1999) or the incisional hernia (Lucha et al., 2007) and the strength of soldered tissues (Forer et al., 2007). However, this method has not been used to test the strength of hard tissues, such as bone or teeth.

The aim of the present study was to examine the effect of root morphology, which is one aspect of VRF, on the susceptibility of endodontically treated teeth to VRF, by applying bursting pressure to two groups of teeth: maxillary central incisors and maxillary premolars.

2. Materials and methods

2.1. Teeth

A total of 48 intact teeth (30 maxillary incisors and 18 maxillary second premolars) that were extracted for periodontal or adult orthodontic reasons from individuals aged < 50 y were included in the main study. In addition, 8 intact central incisors were used in a pilot study conducted to identify an appropriate sealing material. The study protocols were approved by the Tel-Aviv University Ethics Committee, and all patients signed an inform consent form. The teeth were cleaned of soft tissue remnants and/or calculus with hand curettes and then stored in saline that contained 0.01% Thymol (Sigma-Aldrich, Rehovot, Israel) at 5 °C until the experiment. Radiographs were used in the buccal-lingual and mesial-distal projections to verify the presence of a single patent root canal. Teeth were inspected for pre-existing root cracks using trans-illumination (Sendolight, Sjoding Sendoline, Kista, Sweden) under a stereomicroscope at X20 magnification (Wild W-8, Heerbrugg, Switzerland) (Wilcox et al., 1997). The samples that presented cracks were omitted from the study. Teeth that fulfilled all of the inclusion criteria were used within 2 weeks of extraction. All teeth were digitally photographed before and after mechanical testing (Coolpix 500, Nikon).

2.2. Root canal preparation

To obtain a flat surface, the occlusal surfaces were horizontally reduced by 2 mm using a diamond disc under an air-water spray. Endodontic access cavities were prepared, the canals were negotiated with #15 K files, and a working length that was 1 mm short of the apical foramen was established. Root canals were prepared using ProFile files (Dentsply-Maillefer, Ballaigue, Switzerland) to #35/.04, which were operated at 300 rpm to the working length, and the apical 2–3 mm was then further prepared sequentially with K files (Zipperer, Dentsply-DeTrey) to #50. RC-Prep (Premier, Philadelphia, PA, USA) was used with each instrument, and irrigation with 1 ml of 3% sodium hypochlorite was applied after each instrument was used. The canals were then dried using paper points. At all times until experimentation, the outer surface of the tooth was maintained at 100% humidity by wrapping with wet gauzes, and the moisture of the inner surface of the root was maintained by the continuous presence of saline in the canal.

2.3. Mounting of teeth for the bursting pressure experiment

Stainless steel mounting plates were fabricated for tooth mounting. The plate consisted of two combined 2 mm thick flattened cylinders with outer diameters of 22 and 16 mm. Two cannulas (6 and 4 mm long) extended from the outer surfaces of the smaller and larger cylinders, respectively, and each cannula had outer and inner diameters of 1.25 and 1.0 mm, respectively (Fig. 1). The longer (internal) cannula was connected to the access cavity of the tooth, and the shorter (external) cannula was connected to the pressurization apparatus. The longer cannula was bonded into the access cavity of the crown with industrial acrylic cement (Penloc, Panacal, Switzerland). This cement was chosen after the pilot study, which was conducted to test the four sealing systems (each per 2 pilot teeth): A) the dentin was treated by total etch and bonding resin (One-step, Bisco, Itasaca, IL), the sealing material consisted of flowable resin cement (Elitflo, Bisco, Itasaca, IL), and the metal surface received no treatment; B) the dentin was treated as in A but the metal surface was sandblasted with 50 μm aluminum oxide particles (Sandblaster, Ronvig, Oslo, Norway); C) the dentin was treated as in A but the metal surface received tribochemical coating (Cojet, 3M ESPE, Seefeld, Germany); and D) Penloc sealing material was applied to both the dentin and metal surfaces. The first three systems achieved sealing capabilities of < 6 MPa (see Section 2.5), whereas the Penloc sealing material achieved a sealing capability of ≥26 MPa and thus was defined as the material of choice.

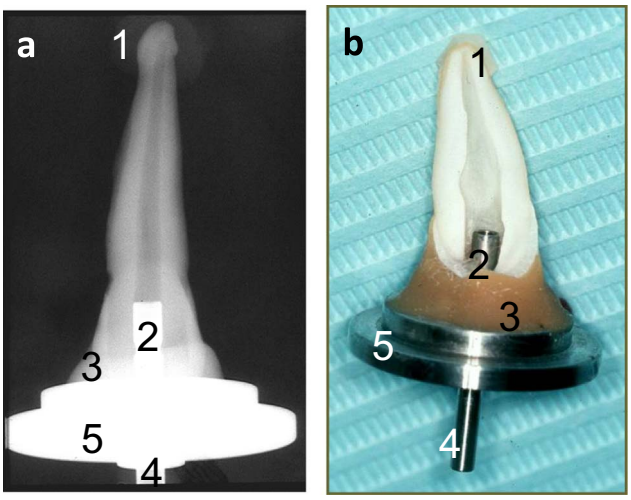

Fig. 1. (a) Radiograph and (b) digital photograph of a mounted maxillary central incisor. 1. Flowable composite resin sealing the apex. 2. Internal cannula bonded into the access cavity. 3. Penloc acrylic cement sealing the access cavity. 4. External cannula connecting the mounting plate to the pressure generating system. 5. Inner and outer flattened cylinders from which the inner and outer cannulas extrude.

A no. 60 file was passed through the cannula verify its patency. The apical end of the root canal was surface treated with 37% phosphoric acid and bonding resin (One Step, Bisco, Itasaca, IL, USA) according to the manufacturer's instructions and then sealed with flowable composite resin (Elitflo, Bisco, Itasaca, IL, USA).

2.4. Bursting pressure experiment

The pressure generating system (Fig. 2) consisted of a water-filled piston that was connected to a universal loading machine (Fig. 2a) (Instron, Model 4502, Buckinghamshire, England), and its exhaust port was connected to a T-splitter (Fig. 2b) that had three ports: one connected to the piston, one connected to the external cannula attached to the tooth and one connected to a pressure transducer (Bosch, Germany) and a display (Red Lion, Chesterfield, UK). The loading machine and the pressure transducer were connected to a computer for on-line data acquisition (Test Point, Keitley, USA). A protective transparent bursting chamber, which consisted of a base and a transparent Perspex cover screwed onto the base, was used. The mounting plate (with its external cannula) was fitted and tightened onto the base with a threaded bolt.

By loading the piston during the compression, the pressure gradually increased through the external cannula into the root canal. Extra care was taken to avoid incorporating air into the system by first filling the root canal and access cavities with water via a 22 G needle through the cannula, starting at the apical terminus of the canal until the canal's cavity was filled with water and excess water drops were observed at the external cannula's orifice. Then, the tooth with its mounting plate was connected to the base of the bursting chamber, and a rubber seal ("O ring") was added onto the external cannula that was connected to the pressure system and the mounting plate was fixed with a nut. The piston was compressed by the loading machine with a cross-head speed of 1.0 mm/min simultaneously with the acquisition of pressure data at 10 Hz.

Vertical root fracture was observed when water burst from the root surface with or without evident root splitting (Fig. 3a) along with a concomitant abrupt drop in pressure.

2.5. Analysis

Failure classification was immediately determined by either evident root fracture, in which the splitting of the root was clearly observed (Fig. 3a, b), or by the presence of cracks (Fig. 3c). These cracks were further analyzed via trans-illumination. For the exact measurement of root wall thickness and identification of the location of resulting cracks, each tooth was stained and sectioned (see below). In samples that exhibited root splitting, the original morphology was restored by assembling the fractured segments with sticky wax.

Each tooth was disassembled from the mounting plate, immersed for 24 h in 0.5% Basic Fuchsine, and then rinsed in water and wiped with 10% ethanol. Each root was then embedded in a Teflon mold that was filled with clear acrylic resin (Justi's Quick Resin, Premier, USA). After 24 h, parallel root slices were cut 1.5 mm apart and perpendicular to the root longitudinal axis (Isomet Plus Low Speed Saw, Buehler LTD, Lake Bluff, IL, USA). These sections were digitally photographed using a binocular microscope X12, (Wild, Heerbrugg, Switzerland). Cracks were defined as bilateral or unilateral when they extended from the root canal to two or one external surfaces, respectively. Measurements were performed from the mid-root slice at X8 magnification (Tool Maker Microscope Mitutoyo, Tokyo, Japan). The mid-root slice, which represents the mid-distance between the CEJ and the root apex, was chosen as a representative slice because all of the failures involved in that region. Fine pencil marks were placed on that slice to represent the buccal-lingual and mesial-distal axis, and the measurements followed those marks. The following morphometric parameters of each root were measured: root canal wall thickness (buccal, lingual, mesial, and distal), diameter of the root canal (buccal-lingual and mesial-distal), total proximal (mesial-distal) and buccal-

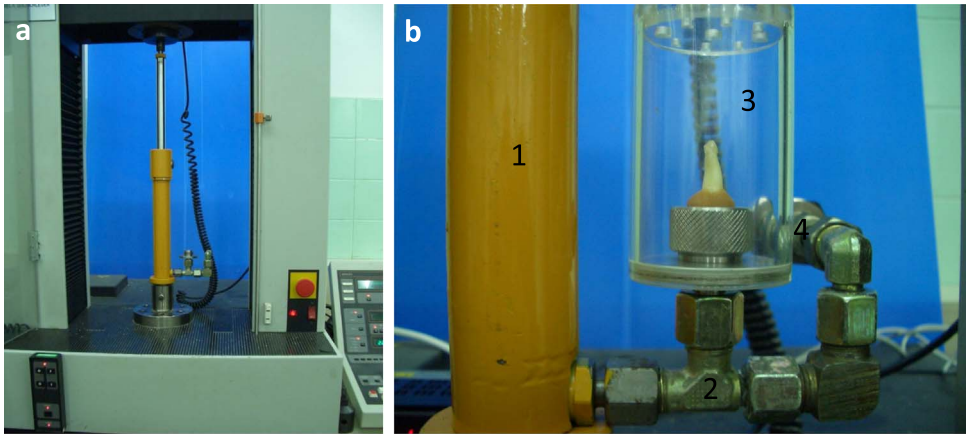

Fig. 2. Pressure generating system. (a) Piston filled with water connected to a universal loading machine. By loading the piston under compression, the pressure increased and the water was forced through the splitter into the external cannula that was bonded into the root canal. (b). Bursting chamber containing the mounted tooth. 1. Piston. 2. T-splitter. 3. Transparent bursting chamber. 4. Pressure transducer.

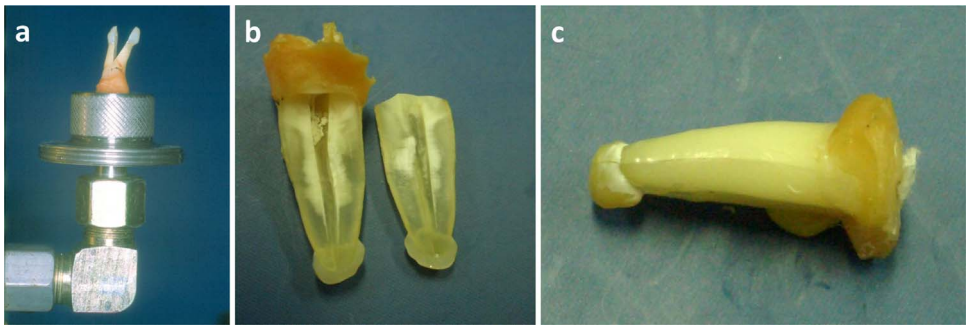

Fig. 3. Failure was classified as (a, b) evident vertical root fracture with splitting of the root and (c) cracking.

lingual root thickness, and ratios (buccal-lingual/mesial-distal) of the total root as well as root canal diameters.

2.6. Statistics

Comparisons between the bursting pressure and the morphometric parameters in the central incisors vs. the second premolars were conducted using unpaired t-tests. Correlations between the bursting pressure and the morphometric parameters were analyzed by Pearson's correlation coefficient. Analyses of Covariance were used to compare the bursting pressure of the incisors vs. premolars and conducted for the following covariates: root canal wall thickness (buccal, lingual, mesial, and distal), total proximal wall thickness, and the ratios (buccal-lingual/mesial-distal) of the total root as well as root canal diameters. Differences were considered significant at $p < 0.05$.

3. Results

Of the 48 studied teeth, water leakage occurred at a mean pressure value of 6.6 ± 1.3 MPa at the interphase between the Penloc sealing material and the mounting plate in 7 teeth (5 incisors and 2 premolars). These teeth were discarded from the study group because they represented a failure in sealing. In the remaining 41 teeth (25 central incisors and 16 second premolars), the failure manifested as either evident VRF (44%) with a visible separation of root fragments or a crack without a visible separation of root fragments (56%). In the latter cases, water could be observed somewhere on the root surface when the maximal pressure value (=bursting pressure) was achieved. The final diagnosis of a crack was performed via trans-illumination, and the diagnosis was finally confirmed after sequential sectioning. Teeth originated from periodontal or orthodontic reasons gave similar results, so no subdivision to the results of the two sources is presented.

Fig. 4 presents two patterns of pressure vs. time during loading curves. The first was a curve with a constant slope, and the experiment ended in an evident VRF with an immediate drop of pressure; the second was a bi-modal curve, and the experiment ended in a crack. The first curve was observed in most of the experimental samples, whereas the second pattern was evident in only 5 teeth, which were diagnosed as cracked. All experiments ended in an abrupt decline in pressure values. No significant differences were found in the bursting pressures between the evident VRF and cracked root groups (21.6 ± 7.5 MPa and 23.3 ± 4.4 MPa, respectively, p=0.62); therefore, the two groups were united and the bursting pressure was considered the dependent variable for further analysis. Bursting pressure was significantly lower in premolars compared with incisors (19.1 ± 3.3 MPa and 25.5 ± 4.5 MPa, respectively, p=0.001, Table 1).

Cracked roots have three morphometric appearances as evidenced via trans-illumination, and they were subsequently approved by sequential sectioning: apex to CEJ (61%), apex to mid-root (26%) and mid-root to CEJ (13%). Evident VRF involved two surfaces, and the roots that were categorized as cracked involved either two surfaces (52%) (Fig. 5) or one surface (48%) (Fig. 6).

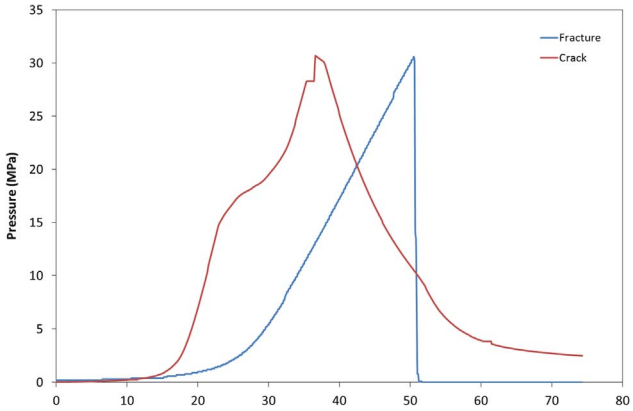

Fig. 4. Two patterns of pressure vs. time until failure curves. The curve with the constant slope ended in evident VRF; and the second curve with a bimodal appearance ended in a crack.

Table 1
Comparison between incisors and premolars in bursting pressure (MPa) and root morphometric parameters (mm).

Parameter	Tooth	No. of teeth	Mean (SD)		P value
Bursting pressure (MPa)	Incisor	25	25.5	(4.5)	0.001*
	Premolar	16	19.1	(3.3)	
Buccal wall thickness	Incisor	25	2.16	(0.56)	0.56
	Premolar	16	2.05	(0.54)	
Lingual wall thickness	Incisor	25	2.38	(0.39)	0.28
	Premolar	16	2.23	(0.45)	
Buccal-lingual root canal diameter	Incisor	25	1.35	(0.57)	0.09
	Premolar	16	1.73	(0.81)	
Mesial wall thickness	Incisor	25	1.65	(0.32)	0.001*
	Premolar	16	1.24	(0.27)	
Distal wall thickness	Incisor	25	1.68	(0.26)	0.001*
	Premolar	16	1.31	(0.23)	
Mesial-distal root canal diameter	Incisor	25	1.05	(0.38)	0.28
	Premolar	16	0.92	(0.35)	
Total buccal+lingual root thickness	Incisor	25	5.89	(0.90)	0.64
	Premolar	16	6.02	(0.72)	
Total mesial+distal root thickness	Incisor	25	4.38	(0.57)	0.001*
	Premolar	16	3.47	(0.37)	
Ratio of total root dimensions[a]	Incisor	25	1.36	(0.26)	0.001*
	Premolar	16	1.75	(0.29)	
Ratio of canal dimensions[a]	Incisor	25	1.35	(0.59)	0.012*
	Premolar	16	1.94	(0.84)	

[a] Ratio refers to dimensions in the buccal-lingual aspect divided by the dimensions in the mesial-distal aspect.
* Significant values ($p < 0.05$).

The main pattern of failure involved the buccal and lingual surfaces together (56%) followed by the buccal (20%) or lingual (7%) surfaces alone (Fig. 7). The buccal surface was involved in 83% of the failures, whereas the lingual surface was involved in 63% of failures, which was followed by the mesial (15%) and distal (5%) surfaces.

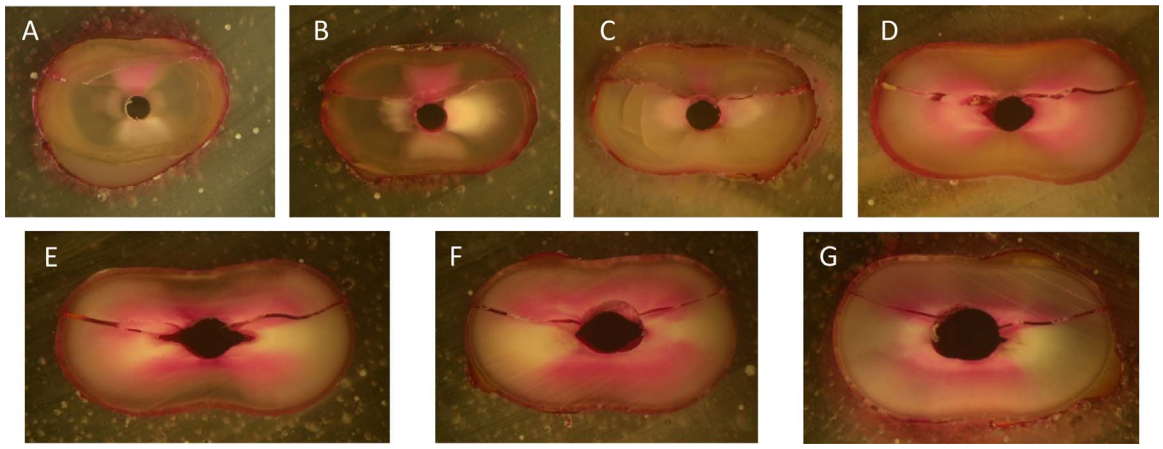

Fig. 5. Cross sections of a root with cracks involving two surfaces (buccal+lingual). The sections presented are 1.5 mm (a), 3.0 mm (b), 4.5 mm (c), 6 mm (d), 7.5 mm (e), 9.0 mm (f) and 10.5 mm (g) from the apex. Other sections with an identical appearance are not presented.

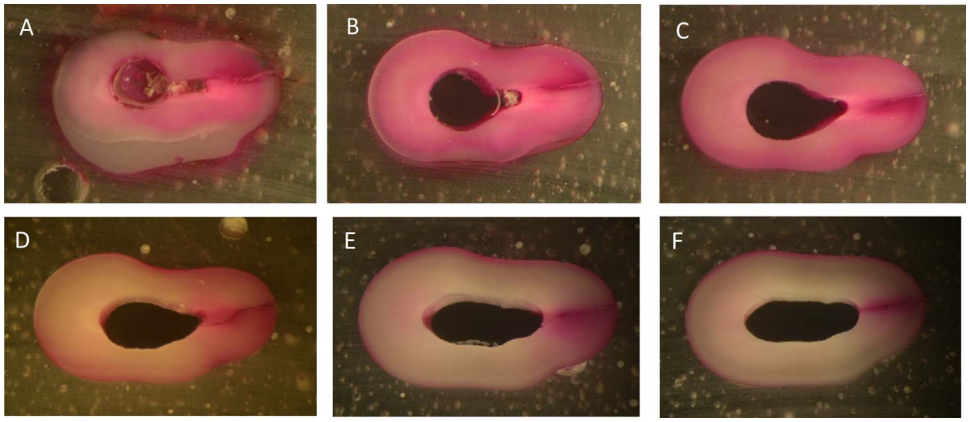

Fig. 6. Cross sections of a root with cracks present on one surface (buccal). The sections presented are 3.0 mm (a), 4.5 mm (b), 6 mm (c), 9.0 mm (d), 10.5 mm (e) and 13 mm (f) from the apex. Other sections with an identical appearance are not presented.

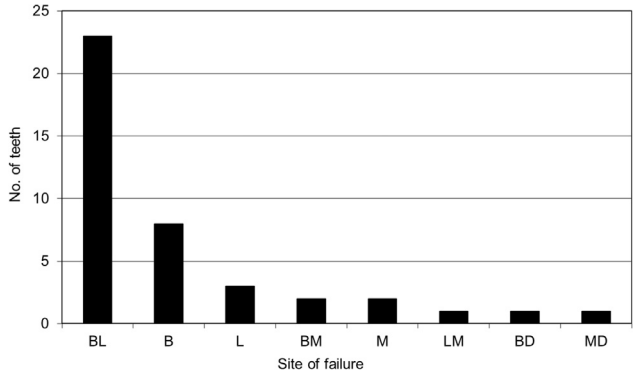

Fig. 7. Classification of failure according to the site (=surfaces involved). B=buccal, L=lingual, M=mesial, and D=distal.

Table 1 compares the morphometric parameters of the central incisors vs. second premolars as obtained from the mid-root sections. Incisors were characterized by higher mesial and distal wall thickness as well as total proximal (mesial+distal) root thickness compared with the premolars ($p < 0.001$). No significant differences were detected in the same parameters of the buccal-lingual aspect (buccal, lingual and total buccal+lingual root thickness) ($p \geq 0.28$). The root canal was more oval shaped in the premolars than in the incisors and was characterized by higher buccal-lingual to mesial-distal canal diameter ratios: 1.94 ± 0.84 and 1.35 ± 0.59 in the premolars and incisors, respectively ($p=0.012$). The parameters that differentiated the incisors from the premolars were significantly correlated with the bursting pressure

Table 2
Correlations between the bursting pressure and morphometric parameters.

Morphometric parameter	r	p
Buccal wall thickness	0.010	0.953
Lingual wall thickness	0.069	0.668
Buccal-lingual root canal diameter	−0.384	0.013*
Mesial wall thickness	0.306	0.049*
Distal wall thickness	0.524	0.001*
Mesial-distal root canal diameter	−0.057	0.724
Total buccal+lingual root thickness	−0.281	0.075
Total mesial-distal root thickness	0.374	0.016*
Ratio of total root dimensions[a]	−0.471	0.002*
Ratio of canal dimensions[a]	−0.303	0.054

[a] Ratio refers to dimensions in the buccal-lingual aspect divided by the dimensions in the mesial-distal aspect.
* Significant values ($p < 0.05$).

(Table 2). Positive correlations were observed between the bursting pressure and mesial ($r=0.306$, $p=0.049$), distal ($r=0.524$, $p=0.001$) and total proximal root wall thickness ($r=0.374$, $p < 0.016$), and negative correlations were observed between the bursting pressure and the ratios (buccal-lingual/mesial-distal) of the total root ($r=-0.471$, $p < 0.002$) and canal ($r=-0.303$, $p=0.054$) dimensions. Buccal or lingual wall thicknesses were not significantly different between the incisors and premolars and did not exhibit significant correlations with the bursting pressure ($p \geq 0.668$). The Analyses of Covariance showed that significant differences in bursting pressure still occurred between the premolars and incisors when the buccal or lingual wall thicknesses were considered as covariates ($p \leq 0.012$). However, when the mesial,

distal or mesial+distal root wall thicknesses were considered as covariates, significant differences were not observed in the bursting pressure (p=0.064, p=0.751 and p=0.113, respectively) between the incisors and premolars. When the ratio of the total root or canal cross-sectional dimensions (buccal-lingual/mesial distal) was considered as a covariate, significant differences were observed in the bursting pressure between the premolars and incisors (p=0.045 and p=0.049, respectively).

4. Discussion

The bursting pressure methodology was applied for the first time to test the strength of human hard tissues, such as bone or teeth, and it was applied in the current study to evaluate recently extracted normal teeth after a root canal preparation. This approach was able to avoid the complex and less readily defined mechanical environment that is typically created in the common external or internal load-to-fracture experiments. (Capar et al., 2014; Lertchirakarn et al., 1999, 2003a; Nur et al., 2015; Sathorn et al., 2005a). Furthermore, this method was able to overcome issues that prevented the full interpretation of previous experiments, such as uneven stress distribution, loading direction and spreader type (Lertchirakarn et al., 1999, 2003a; Lindauer et al., 1989; Sathorn et al., 2005a).With the bursting pressure methodology, the hydrostatic pressure was dispersed evenly throughout the endodontic cavity and uniformly applied to the root canal walls. All of the problems that could influence the failure of the root, such as the inhomogeneity and anisotropy of the dentin, the complex spatial and anatomy variations (Bellucci and Perrini, 2002; Brauer et al., 2010; Xu et al., 2014), potential defects induced during canal preparation (El Nasr and El Kader, 2014; Rippe et al., 2014) and intrinsic cracks (Kinney et al., 2003), were reflected in the outcome obtained via the new method, yielding the true strength of the roots. It might be argued that the sealed apex does not correspond to the in vivo situation. However as the apical sealing was identical to premolars and incisors, the comparison is valid. Moreover, when VRF occurred it involved the bonding resin at the apex like an extension of the root without changing the pattern of the VRF (Figs. 1 and 3).

The current study demonstrates that the bursting pressure of maxillary central incisors was 34% higher than that of the maxillary premolars, whereas the difference reported with the use of increased load to failure experiments, which exerted stress unevenly, was 100% (Lertchirakarn et al., 1999). As an initial approximation, the roots can be regarded as thick-walled pressure vessels that are subject to internal pressure p_1. The resultant stresses are circumferential (hoop) tensile (S_t) and radial compressive (S_r). According to Lame's equations (Avallone et al., 1996), in an equilibrium state, these stresses at a variable distance (r) are:

$$S_t = \frac{r_1^2 p_1 - r_2^2 p_2 + (p_1 - p_2)\frac{r_1^2 r_2^2}{r^2}}{r_2^2 - r_1^2} \tag{4.1}$$

$$S_r = \frac{r_1^2 p_1 - r_2^2 p_2 - (p_1 - p_2)\frac{r_1^2 r_2^2}{r^2}}{r_2^2 - r_1^2} \tag{4.2}$$

where S_t denotes the tangential stress; S_r. the radial stresses; r_1 the internal radius; r_2 the external radius; and p_2 denotes the external pressure. The external pressure is negligible compared with the internal pressure and can be set as zero. Therefore:

$$S_t = \frac{r_1^2 p_1}{r_2^2 - r_1^2}\left(1+\frac{r_2^2}{r^2}\right) \tag{4.3}$$

$$S_r = \frac{r_1^2 p_1}{r_2^2 - r_1^2}\left(1-\frac{r_2^2}{r^2}\right) \tag{4.4}$$

When $r=r_1$, the stresses will be maximal, which implies that the maximal tensile and radial compressive stresses are acting on the internal surface of the root:

$$S_{tmax} = \frac{p_1(r_2^2 + r_1^2)}{r_2^2 - r_1^2} \tag{4.5}$$

$$S_{rmax}=-p_1 \tag{4.6}$$

The aforementioned model is an oversimplification of the real anatomy as follows: (1) the endodontic cavity is elliptically shaped as observed in cross-sections, and the observed buccal-lingual (major axis) to mesial-distal (minor axis) canal ratios were 1.35 and 1.94 in the central incisors and premolars, respectively; and (2) the wall of the cylinder is not uniformly thick and thinner in the mesial-distal axis (4.38 mm and 3.47 mm in the incisors and premolars, respectively) and thicker in the buccal-lingual axis (5.89 mm and 6.02 mm in the incisors and premolars, respectively) (Table 1).

If the semi-minor and semi-major axes are designated as a and b, respectively, and the ellipse is subjected to internal pressure p_1, then bending moments will develop in the circumference of the ellipse (Avallone et al., 1996). This moment will be minimal *(Mo)* in the region where the radius of the curvature is maximal (mesial-distal axis), and its magnitude will be determined according to the following equation:

$$M_0 = \frac{p_1 a^2}{2} - \frac{p_1 I_x}{2S} - \frac{p_1 I_y}{2S} \tag{4.7}$$

where I_x denotes the moment of inertia of the quarter ellipse arc in the x axis (mesial-distal); I_y denotes the moment of inertia of the quarter ellipse arc in the y axis (buccal-lingual); and S denotes the stress.

This moment will be maximal (M_{max}) where the radius of the curvature is minimal (buccal-lingual axis), and its magnitude will be determined according to the following equation:

$$M_{max} = M_0 - \frac{p_1(a^2 - b^2)}{2} \tag{4.8}$$

Referring to the first deviation from the classic model of the thick-walled cylinder, the conclusion is that when the root is more elliptical in cross section (premolars), the bending moments are maximal at the buccal-lingual plane, where the radius of the curvature is minimal, thereby resulting in the highest tangential stresses in this zone. This conclusion is consistent with the findings reported by Lertchirakarn et al. (2003a, 2003b) as well as by Sathorn et al. (2005b), who used FEA models. When the canal shape and the external root cross-sectional shape are elliptical instead of circular, the intra-canal stress distribution becomes asymmetrical, and the highest stresses tend to occur in the buccal-lingual direction on the inner-canal wall.

The second deviation from the classic model was previously investigated by Lertchirakarn et al. (2003a, 2003b), who demonstrated in an FEA model that a reduced proximal dentin thickness increases the magnitude of the stresses, and when the thickness is equal to 0.5 mm, the resulting buccal-lingual stresses are 175% higher than those of the simple thick wall cylinder model (Lertchirakarn et al., 2003a, 2003b).

Theoretical and FEA models require validation. The current study validates the theoretical (Chai and Tamse, 2015) and FEA studies (Lertchirakarn et al., 2003a, 2003b) by showing that when the buccal or lingual wall thickness was considered as a covariate, a significant difference in bursting pressure still occurred between the premolars and incisors. However, when the proximal root wall thickness was considered a covariate, significant differences were not observed in the bursting pressure between the incisors and premolars. When the ratio of the total root or canal cross-sectional dimensions (buccal-lingual/mesial distal) were considered as covariates, the current study could not eliminate the significant differences in bursting pressure between the premolars and incisors; however, although significant differences occurred, the level of significance increased from 0.001 and ap-

proached borderline values (p=0.045 and p=0.049 for the ratio of the total root or the canal cross-section, respectively). An increase in the sample number might lead to insignificant values, which indicates that the proximal wall thickness and elliptical root cross-sectional shape are the variables that determine the differences in strength between premolars and incisors.

The highest pressures that were previously achieved in bursting pressure experiments of living organs were those obtained for bovine caudal disk samples and ranged from 15 to 22 MPa (Schechtman et al., 2006). Normal central incisors or first premolars withstood higher pressures ranging from 15 to 32 MPa. The sealing material in the current study would therefore have to withstand pressures of > 30 MPa. Our results indicated that the interface of metal (internal cannula) and dentin (access cavity) was difficult to seal. Metal surface treatments, such as sandblasting or tribochemical coating combined with resin composite sealer, failed to withstand more than 6 MPa of pressure. However, the Penloc sealing material succeeded in withstanding more than 26 MPa in the pilot study. Penloc is an acrylic-based high-performance structural adhesive. As per the manufacturer's recommendations, whenever the gap size is > 0.3 mm, the adhesive should be dispensed directly from the static mixer. The incorporation of bubbles at the interphase of the mounting plate and the Penloc are assumed to account for the sealing failures that occurred at ~6 MPa in the 7 teeth that were discarded from the main study.

An age group of < 50 y was chosen to minimize the effect of age as a possible confounding factor. Old dentine (50–80 y) showed a greater hardness, a higher elastic modulus and a greater mineral content compared with young dentine (Xu et al., 2014). Greater susceptibility to fracture was reported for premolars in the age group > 60 y compared with the age group 18–21 y (de Noronha et al., 2012).

The resulting failures observed in the present study consisted of either evident VRF with a visible separation of fragments or a crack that was diagnosed and confirmed by trans-illumination and sequential sectioning. As the bursting pressures of these two modes did not differ significantly, it appears that this classification is artificial; thus, they can both be regarded as VRF. Previous studies have shown that VRF appears to be caused by pre-existing flaws that cause teeth to fail at stresses that are far lower than their theoretical strength (Kinney et al., 2003; Rippe et al., 2014). The presence of an endodontic preparation appears to be one of the factors that can generate irregularities in the root canal, mostly at the apical region (Capar et al., 2014, 2015; Helvacioglu-Yigit et al., 2015; Rippe et al., 2014). When the sequential sections in all the failures categorized as one-sided cracked roots are evaluated, it demonstrated irregularities on one surface or differences in canal curvature between the different aspects of the root, mainly between the buccal and lingual aspects (Fig. 6). These irregularities or flaws can become areas of high tensile stress concentration initiating failure (Kinney et al., 2003) and thus might explain the one-sided cracks. Such failures are common in clinical cases of VRF, leading to extensive bone loss before diagnosis (Tamse et al., 1999; Yoshino et al., 2014), but are not completely mimicked in the conventional destructive tests. In contrast, when pressure was applied during the bursting pressure experiment, the progression to catastrophic VRF was anticipated at surfaces with irregularities or a greater canal curvature (=minimal radius of curvature). FEA models have indicated that the canal curvature appeared to be more important than the external root morphology in terms of stress concentration (Lertchirakarn et al., 2003a). The progression of water under pressure from the inner canal compartment to the external surface implies the presence of a VRF, which may be categorized as an evident VRF or a crack.

The main pattern of pressure vs. time curve consisted of a constant slope that started after a lag phase as the pressure developed in the system, and it ended in abrupt failure. In the 5 tested roots that exhibited a different bi-modal curve pattern, cracks likely occurred during the steep slope, which did not pass abruptly through all of the root wall thicknesses but arrived at an external location and was subsequently followed by a toughening mechanism during crack growth. This toughening is greatest in the outer dentin (Ivancik and Arola, 2013). With further increases in pressure, the cracks propagate, which was observed because of water leakage along the root.

5. Conclusions

The bursting pressure methodology can be applied to test the strength of endodontically treated teeth. The outcome of bursting pressure is VRF. This approach avoids the complex and less readily defined mechanical environment that is created in common load-to-fracture experiments. The bursting pressure of maxillary central incisors is 34% higher than that of the maxillary premolars. The proximal wall thickness and elliptical root cross-sectional shape are the variables that determine the differences in strength between premolars and incisors. Cracks can involve two surfaces or one surface. Irregularities on one surface or differences in canal curvature between the different aspects of the root, mainly between the buccal and lingual aspects are associated mainly with one-sided cracks.

Disclosures

The authors have no conflicts of interest to declare.

Financial support

This research did not receive any specific grant from funding agencies in the public, commercial or not-for-profit sectors.

References

Avallone, E.A., Baumeister, T., III, Sadegh, A.M., 2007. Marks' Standard Handbook for Mechanical Engineers, chapter 5 eleventh ed. McGraw-Hill Co, New York, 45–47.
Bellucci, C., Perrini, N., 2002. A study on the thickness of radicular dentine and cementum in anterior and premolar teeth. Int. Endod. J. 35, 594–606.
Brauer, D.S., Marshall, G.W., Marshall, S.J., 2010. Variations in human DEJ scallop size with tooth type. J. Dent. 38, 597–601.
Capar, I.D., Altunsoy, M., Arslan, H., Ertas, H., Aydinbelge, H.A., 2014. Fracture strength of roots instrumented with self-adjusting file and the protaper rotary systems. J. Endod. 40, 551–554.
Capar, I.D., Saygili, G., Ergun, H., Gok, T., Arslan, H., Ertas, H., 2015. Effects of root canal preparation, various filling techniques and retreatment after filling on vertical root fracture and crack formation. Dent. Traumatol. 31, 302–307.
Chai, H., Tamse, A., 2015. The effect of isthmus on vertical root fracture in endodontically treated teeth. J. Endod. 41, 1515–1519.
de Noronha, F., Scelza, M.F.Z., da Silva, L.E., de Carvalho, W.R., 2012. Evaluation of compressive strength in the first premolars between young and elderly people: ex vivo study. Gerodontology 29, e898–e901.
Eker, T., Genc, V., Sevim, Y., Cumaogullari, O., Ozcelik, M., Kocaay, A.F., Ensari, C.Ö., Pasaoglu, O.T., 2015. The effects of ventilation with high density oxygen on the strength of gastrointestinal anastomosis. Ann. Surg. Treat. Res. 89, 17.
El Nasr, H.M., El Kader, K.G., 2014. Dentinal damage and fracture resistance of oval roots prepared with single-file systems using different kinematics. J. Endod. 40, 849–851.
Fallon, E.M., Nehra, D., Carlson, S.J., Brown, D.W., Nedder, A.P., Rueda, B.R., Puder, M., 2014. Evaluation of anastomotic strength and drug safety after short-term sunitinib administration in rabbits. J. Surg. Res. 187, 101–106.
Forer, B., Vasileyev, T., Gil, Z., Brosh, T., Kariv, N., Katzir, A., Fliss, D., 2007. CO(2) laser fascia to dura soldering for pig dural defect reconstruction. Skull Base 17, 17–23.
Haueisen, H., Gärtner, K., Kaiser, L., Trohorsch, D., 2013. Heidemann, vertical root fracture: prevalence, etiology, and diagnosis. Quintessence Int. 44, 467–474.
Helvacioglu-Yigit, D., Aydemir, S., Yilmaz, A., 2015. Evaluation of dentinal defect formation after root canal preparation with two reciprocating systems and hand instruments: an in vitro study. Biotechnol. Biotech. Equip. 29, 368–373.
Holcomb, J.Q., Pitts, D.L., Nicholls, J.I., 1987. Further investigation of spreader loads required to cause vertical root fracture during lateral condensation. J. Endod. 13, 277–284.
Ikeuchi, D., Onodera, H., Aung, T., Kan, S., Kawamoto, K., Imamura, M., Maetani, S., 1999. Correlation of tensile strength with bursting pressure in the evaluation of intestinal anastomosis. Dig. Surg. 16, 478–485.
Ivancik, J., Arola, D.D., 2013. The importance of microstructural variations on the fracture toughness of human dentin. Biomaterials 34, 864–874.
Kinney, J.H., Marshall, S.J., Marshall, G.W., 2003. The mechanical properties of human dentin: a critical review and re-evaluation of the dental literature. Crit. Rev. Oral. Biol. Med. 14, 13–29.
Lertchirakarn, V., Palamara, J., Messer, H., 2003a. Finite element analysis and strain-

gauge studies of vertical root fracture. J. Endod. 29, 529–534.
Lertchirakarn, V., Palamara, J., Messer, H., 2003b. Patterns of vertical root fracture: factors affecting stress distribution in the root canal. J. Endod. 29, 523–528.
Lertchirakarn, V., Palamara, J.E.A., Messer, H.H., 1999. Load and strain during lateral condensation and vertical root fracture. J. Endod. 25, 99–104.
Lindauer, P.A., Campbell, A.D., Hicks, M.L., Pelleu, G.B., 1989. Vertical root fractures in curved roots under simulated clinical conditions. J. Endod. 15, 345–349.
Lucha, P.A., Jr, Briscoe, C., Brar, H., Schneider, J.J., Butler, R.E., Jaklic, B., Francis, M., 2007. Bursting strength evaluation in an experimental model of incisional hernia. Am. Surg. 73, 722–724.
Meira, J.B.C., Quitero, M.F.Z., Braga, R.R., Placido, E., Rodrigues, F.P., Lima, R.G., Ballester, R.Y., 2008. The suitability of different FEA models for studying root fractures caused by wedge effect. J. Biomed. Mater. Res. A 84A, 442–446.
Meister, F., Lommel, T.J., Gerstein, H., 1980. Diagnosis and possible causes of vertical root fractures. Oral. Med. Oral. Pathol. 49, 243–253.
Mireku, A.S., Romberg, E., Fouad, A.F., Arola, D., 2010. Vertical fracture of root filled teeth restored with posts: the effects of patient age and dentine thickness. Int. Endod. J. 43, 218–225.
Nur, B., Ok, E., Altunsoy, M., Tanriver, M., Capar, I., 2015. Fracture strength of roots instrumented with three different single file systems in curved root canals. Eur. J. Dent. 9, 189.
Pilo, R., Kaffe, I., Amir, E., Sarnat, H., 1987. Diagnosis of developmental dental anomalies using panoramic radiographs. ASDC J. Dent. Child. 54, 267–272.
Pitts, D.L., Matheny, H.E., Nicholls, J.I., 1983. An in vitro study of spreader loads required to cause vertical root fracture during lateral condensation. J. Endod. 9, 544–550.
Rippe, M.P., Santini, M.F., Bier, C.A.S., Baldissara, P., Valandro, L.F., 2014. Effect of root canal preparation, type of endodontic post and mechanical cycling on root fracture strength. J. Appl. Oral. Sci. 22, 165–173.
Rivera, E.M., Yamauchi, M., 1993. Site comparisons of dentine collagen cross-links from extracted human teeth. Arch. Oral. Biol. 38, 541–546.
Sathorn, C., Palamara, J., Messer, H., 2005a. A comparison of the effects of two canal preparation techniques on root fracture susceptibility and fracture pattern. J. Endod. 31, 283–287.
Sathorn, C., Palamara, J., Palamara, D., Messer, H., 2005b. Effect of root canal size and external root surface morphology on fracture susceptibility and pattern: a finite element analysis. J. Endod. 31, 288–292.
Schechtman, H., Robertson, P.A., Broom, N.D., 2006. Failure strength of the bovine caudal disc under internal hydrostatic pressure. J. Biomech. 39, 1401–1409.
Seo, D.-G., Yi, Y.-A., Shin, S.-J., Park, J.-W., 2012. Analysis of factors associated with cracked teeth. J. Endod. 38, 288–292.
Sugaya, T., Nakatsuka, M., Inoue, K., Tanaka, S., Miyaji, H., Sakagami, R., Kawamami, M., 2015. Comparison of fracture sites and post lengths in longitudinal root fractures. J. Endod. 41, 159–163.
Tamse, A., Fuss, Z., Lustig, J., Kaplavi, J., 1999. An evaluation of endodontically treated vertically fractured teeth. J. Endod. 25, 506–508.
Tamse, A., Katz, A., Pilo, R., 2000. Furcation groove of buccal root of maxillary first premolars—a morphometric study. J. Endod. 26, 359–363.
Uzun, İ., Arslan, H., Doğanay, E., Güler, B., Keskin, C., Çapar, I.D., 2015. Fracture resistance of endodontically treated roots with oval canals restored with oval and circular posts. J. Endod. 41, 539–543.
Wilcox, L.R., Roskelley, C., Sutton, T., 1997. The relationship of root canal enlargement to finger-spreader induced vertical root fracture. J. Endod. 23, 533–534.
Xu, H., Zheng, Q., Shao, Y., Song, F., Zhang, L., Wang, Q., Huang, D., 2014. The effects of ageing on the biomechanical properties of root dentine and fracture. J. Dent. 42, 305–311.
Yoshino, K., Ito, K., Kuroda, M., Sugihara, N., 2014. Prevalence of vertical root fracture as the reason for tooth extraction in dental clinics. Clin. Oral. Invest. 19, 1405–1409.